

UPDATE ON THE MEIC ELECTRON COLLIDER RING DESIGN*

F. Lin[#], Ya.S. Derbenev, L. Harwood, A. Hutton, V.S. Morozov, F. Pilat, Y. Zhang, Jefferson Lab,
Newport News, VA, USA

Y. Cai, Y.M. Nosochkov, M. Sullivan, M-H Wang, U. Wienands, SLAC, Menlo Park, CA, USA

Abstract

The electron collider ring of the Medium-energy Electron-Ion Collider (MEIC) at Jefferson Lab is designed to accumulate and store a high-current polarized electron beam for collisions with an ion beam. We consider a design of the electron collider ring based on reusing PEP-II components, such as magnets, power supplies, vacuum system, etc. This has the potential to significantly reduce the cost and engineering effort needed to bring the project to fruition. This paper reports on an electron ring optics design considering the balance of PEP-II hardware parameters (such as dipole sagitta, magnet field strengths and acceptable synchrotron radiation power) and electron beam quality in terms of equilibrium emittances.

INTRODUCTION

The electron complex of the MEIC is designed to meet the physics requirements for the project [1]. These include a beam energy range of 3 to 10 GeV, a beam current of 3 A up to an energy above 6 GeV, a short bunch length (approximately 1 cm) and small transverse emittance over a wide energy range to support the luminosity requirement, and a longitudinal polarization of 70% or above at collision points with a reasonably long lifetime. In addition, the linear density of synchrotron radiation power is less than 10 kW/m and the total power less than 10 MW.

The CEBAF 5.5 pass SRF recirculating linac serves as a full energy injector to the MEIC electron collider ring. No further upgrade is needed beyond the current CEBAF 12 GeV upgrade in terms of beam current and polarization (> 85%). In the MEIC baseline design, the PEP-II 476 MHz RF system will be reused in the electron collider ring [2]. To synchronize the RF bucket between CEBAF whose RF frequency is 1497 MHz and the electron collider, we note that 7/22 of the CEBAF linac frequency is 476.3 MHz. This frequency is well within the operational range of the PEP-II 476 MHz cavities and klystrons. Details of the injection concept is discussed in these proceedings [3].

After the last recirculation in the CEBAF, the beam is sent to a transfer line after the north linac [4]. The transfer line between the linac and the MEIC electron collider ring is made of FODO cells with 120° of phase advance using the PEP-II Low Energy Ring (LER) dipoles and quadrupoles. The strengths of dipoles and quadrupoles are

* Notice: Authored by Jefferson Science Associates, LLC under U.S. DOE Contract No. DE-AC05-06OR23177 and DE-AC02-06CH11357. Work also supported by the U.S. DOE Contract No. DE-AC02-76SF00515. The U.S. Government retains a non-exclusive, paid-up, irrevocable, world-wide license to publish or reproduce this manuscript for U.S. Government purposes.

[#] fanglei@jlab.org

well within their specifications. There are a number of reasons to choose a phase advance of 120° . First, it keeps the quadrupole gradients low enough so that the PEP-II LER quadrupoles can be reused. Second, it is compatible with a missing dipole scheme for dispersion suppression. Third, such phase advance insures that there is no significant emittance growth due to synchrotron radiation during the transport of electron beam from the CEBAF to the MEIC electron collider ring. The length of the entire transfer line is approximately 333 m.

The electron and ion collider rings of the MEIC are designed to follow the same footprint and share the same underground tunnel. The electron ring determines the overall geometry that the ion ring follows with the exception of the region around the IP due to the 50 mrad crossing angle. The dimension of the electron ring should be able to accommodate all machine components. This paper presents the electron collider ring optics design using the PEP-II High Energy Ring (HER) magnets.

ELECTRON COLLIDER RING DESIGN

The MEIC electron collider ring is designed as a FODO lattice in both arcs and straights, using the majority of PEP-II dipoles and quadrupoles within the limit of their strengths [5]. Particular machine blocks, such as spin rotators, interaction regions and RF sections etc., are designed as modules using new dipoles and quadrupoles, inserted and matched into the base line lattice.

Each arc has 34 normal FODO cells and 8 matching cells (4 in each end of the arc). The normal FODO cell is 15.2 m long and filled with two 5.4 m long PEP-II dipoles and two 0.56 m long PEP-II arc quadrupoles. Each quadrupole is followed by a PEP-II sextupole for chromatic compensation in the arcs. Though the dipole field strength of 0.3 T at 10 GeV in the MEIC is higher than the 0.27 T shown in [5], PEP-II dipoles can reach 0.363 T because they were originally designed for the PEP 18 GeV electron beam. For the MEIC application, each dipole has a 3.3 cm sagitta based on a bending angle of 2.8° . This sagitta is 1.1 cm larger than the PEP-II dipole sagitta of 2.2 cm, but it is still within the dipole good field region of 5 cm. The matching cell has the same length and magnets of the normal FODO cell, except that the quadrupoles are adjusted to match the optics between the normal FODO cell and the Universal Spin Rotator (USR). The spin rotator is designed with interleaved solenoids and dipoles, and quadrupoles in between for the optics, to rotate the electron polarization between the vertical (in arcs) and longitudinal (at IP) direction from 3 to 12 GeV [6]. Note that the spin rotator does not change the design orbit over the entire range of electron beam energies. The transverse orbital coupling induced by the longitudinal

fields in the solenoids is neutralized by placing quadrupoles between half solenoids. In total, four such spin rotators are located in both ends of two arcs with a bending angle of 13.2° for each of them. Each spin rotator has two 2.5 m long solenoids, two 5 m long solenoids, six 2 m long new dipoles and 21 new quadrupoles (11 families) in order to meet the optics requirements and save space. The optics of a normal arc FODO and matching and USR section is plotted in Fig. 1 and Fig. 2, respectively.

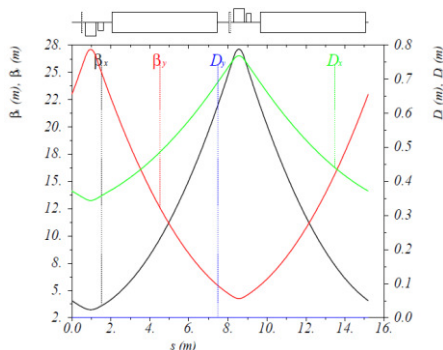


Figure 1: Optics of a normal arc FODO cell in the MEIC electron collider ring.

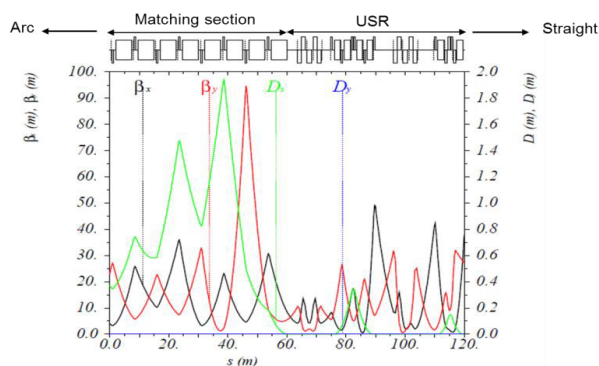


Figure 2: Optics of matching and USR sections in the MEIC electron collider ring.

A dedicated Chromaticity Compensation Block (CCB) has been developed to compensate the chromatic effects induced by the intensively strong focusing at the IP region [7]. In this design approach, the number of aberration conditions at the IP is greatly reduced by requiring certain symmetries of the beam orbital motion and of the dispersion and by utilizing a symmetric arrangement of quadrupoles, sextupoles and/or octupoles with respect to the center of CCB. Such a scheme should allow simultaneous compensation of the 1st-order chromaticities and chromatic beam smear at the IP without introducing significant 2nd-order aberrations. The lattice functions are plotted in Fig. 3. Such a CCB has two 5 m-long dipoles and four 2 m-long dipoles with a maximum field of 0.58 T at 10 GeV, 13 quadrupoles in 7 families with a maximum field gradient of 25 T/m at 10 GeV, and 4 sextupoles in 2 families for the chromaticity

compensation. Except for the sextupoles from the PEP-II, all dipoles and quadrupoles are new magnets.

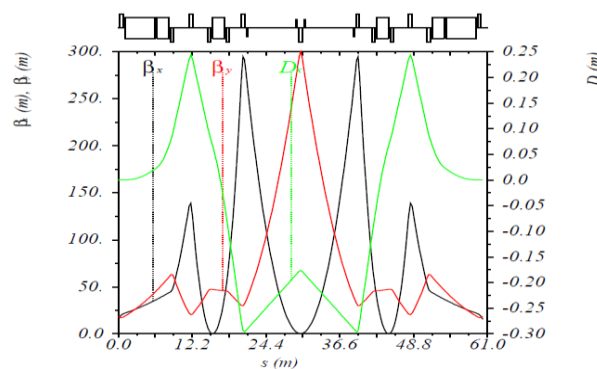


Figure 3: Optics of the Chromaticity Compensation Block (CCB) in the MEIC collider ring.

There are two RF sections in two straights, where the beta functions are designed to be relatively small (5 m) in order to improve the coupled beam instability thresholds. There are 15 quadrupoles in 2 families needed in each section with a maximum field strength of 25 T/m at 10 GeV. The optics of the RF section is plotted in Fig. 4.

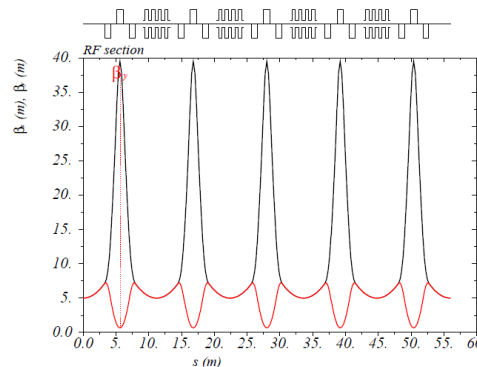


Figure 4: Optics of RF section in the MEIC electron collider ring.

Figure 5 shows the optics of the interaction region that is optimized to meet the detector requirements [8, 9, 10]. The downstream final focusing quadrupoles (FFQs) are designed with large apertures for forward detection and are followed by spectrometer dipoles. Additionally, as shown in Fig. 5, the electron beam is focused again towards the end of the element-free space downstream of the spectrometer dipole to allow closer placement of the detectors at those locations. This, in combination with the relatively large dispersion values there, enhances momentum resolution of the forward detector. The dispersion generated by the spectrometer dipole is suppressed by a simple dipole chicane whose parameters are chosen to avoid a significant impact on the electron equilibrium emittances. It turns out that the center of the chicane is a convenient place for a Compton polarimeter. Because there is no net spin rotation between the polarization measurement point and the interaction point

Content from this work may be used under the terms of the CC BY 3.0 licence (© 2015). Any distribution of this work must maintain attribution to the author(s), title of the work, publisher, and DOI.

(IP), the polarimeter allows for a continuous non-invasive monitoring of the electron polarization at the IP.

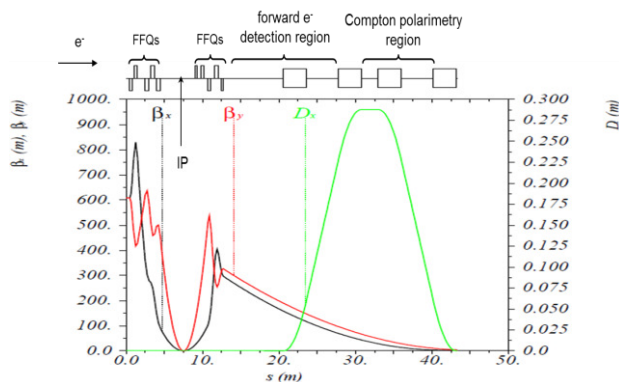


Figure 5: Optics of the detector region in the MEIC electron collider ring.

The geometric layout of the complete figure-8 shape electron collider ring is illustrated in Fig. 6. The circumference of the electron collider is 2154.28m with two identical 754.84 m long arcs and two straights of 322.31 m, respectively. The figure-8 crossing angle is 81.7°. Some high level optics and synchrotron radiation parameters are listed in Tables 1 and 2. The electron currents at high energies are determined by the total synchrotron radiation power of 10 MW within the PEP-II vacuum chamber specification.

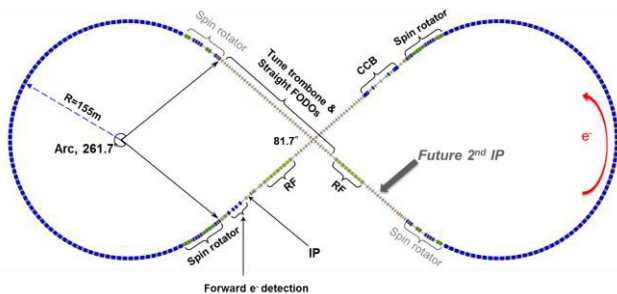


Figure 6: Geometric layout of the figure-8 shape electron collider ring with one IP and major machine sections.

CONCLUSION

The MEIC electron complex is designed to provide high-current polarized electron beams to meet the physics requirements for collisions with ion beams. This paper presents the optics design of the electron collider ring using major PEP-II HER magnets within their specifications. The ring accommodates various machine components for the manipulation of electron polarization and the optimization of single-particle nonlinear beam dynamics together with the detection of forward electrons after collisions.

Table 1: Electron Collider Ring Optics Parameters

Electron beam momentum	GeV/c	10
Circumference	m	2154.28
Arc/Straight length	m	754.84/322.3
Figure-8 crossing angle	deg	81.7
RF frequency	MHz	476
Bunch length	cm	1.6
Beta stars at IP β^*	cm	10/2
Detector space up-/downstream	m	3/3.2
Maximum horizontal/vertical β functions	m	949/692
Maximum horizontal/vertical dispersion $D_{x,y}$	m	1.9/0
Horizontal/vertical betatron tunes $\nu_{x,y}$		45.(89)/43.(61)
Horizontal/vertical chromaticities $\xi_{x,y}$		-149/-123
Momentum compaction factor α		10-3
Transition energy γ_t		21.6
Horizontal/vertical normalized emittance $\epsilon_{x,y}$	$\mu\text{-rad}$	1093/378

Table 2: Synchrotron Radiation Parameters of Electron Beam at Various Energies

Beam energy	GeV	3	5	6.95	9.3	10
Beam current	A	1.4	3	3	0.95	0.71
Total SR power	MW	0.16	2.65	10	10	10
Linear SR power density (arcs)	kW/m	0.16	2.63	9.9	9.9	9.9
Energy loss per turn	MeV	0.11	0.88	3.3	10.6	14.1
Energy spread	10^{-3}	0.27	0.46	0.66	0.82	0.91
Transverse damping time	ms	376	81	26	14	10
Longitudinal damping time	ms	188	41	13	7	5
Normalized emittance	$\mu\text{-rad}$	30	137	425	797	1093

REFERENCES

- [1] S. Abeyratne et al., MEIC Design Report, edited by J. Bisognano and Y. Zhang, arXiv:1209.0757 (2012).
- [2] R. Rimmer et al., in this proceeding, WEPWI024 (2015).
- [3] J. Guo et al., in this proceeding, TUPTY083 (2015).
- [4] S. Abeyratne et al., MEIC Design Summary for NSAC EIC Cost Estimate Sub-Committee, edited by G. A. Krafft, submitted to arXiv (2015).
- [5] M. Bona et al., SuperB CDR, INFN/AE- 7/2, SLAC-R-856, LAL 07-15, March 2007.
- [6] P. Chevtsov et al., JLab-TN-10-026 (2010).
- [7] V.S. Morozov et al., PRST-AB 16, 011004 (2013); arXiv:1208.3405 [physics.acc-ph] (2012).
- [8] V.S. Morozov et al., Proc. of IPAC'12, TUPPR080, p.2011 (2012).
- [9] F. Lin et al., Proc. of IPAC'13, TUPAC28, p.508 (2013).
- [10] V.S. Morozov et al., Proc. of IPAC'14, MOPRO005, p.71 (2014).